

A Rare Case of Dual Emission in a Neutral Heteroleptic Iridium(III) Complex

*Sébastien Ladouceur^a, Loïc Donato^a, Maxime Romain^a, Bhanu P. Mudraboyina^b,
Michael B. Johansen^b, James A. Wisner^{b*} and Eli Zysman-Colman^{a*}.*

^aDépartement de Chimie, Université de Sherbrooke, 2500 Boul. de l'Université, Sherbrooke, QC, Canada, J1K 2R1

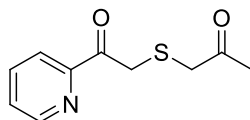
^bDepartment of Chemistry, The University of Western Ontario, 1151 Richmond Street, London, ON, Canada N6A 5B7

<u>Table of Contents</u>	Page
General Procedures for Synthesis	S2
NMR Spectra	S7
Procedure for UPLC-MS and UPLC-MS trace for 2	S11
Procedures for X-Ray Diffraction Measurements	S12
General Procedures for Photophysical Characterization	S16
Supplementary Photophysical Measurements	S19
Procedure for Measurement of O ₂ Quenching and Stern-Volmer Determination	S24
General Procedures for Electrochemical Characterization and CV traces	S25
General Procedures for Thin Film Measurements	S26
Computation Methodology and Supplementary Data	S27
References	S35

General Procedures for Synthesis:

Commercial chemicals were used as supplied. All reactions were performed using standard Schlenk techniques under an inert (N₂) atmosphere. Flash column chromatography was performed using silica gel (Silia-P from Silicycle, 60 Å, 40-63µm). Analytical thin layer chromatography (TLC) was performed with silica plates with aluminum backings (250 µm with indicator F-254). Compounds were visualized under UV light. ¹H and ¹³C NMR spectra were collected on a Varian Mercury 400 MHz spectrometer operating at 400.08 and 100.60 MHz respectively. Spectra are reported with residual solvent peak as reference from TMS. The following abbreviations have been used for multiplicity assignments: “s” for singlet, “d” for doublet, “t” for triplet, “m” for multiplet, and “br” for broad. Deuterated chloroform (CDCl₃) was used as the solvent of record except where noted below. Spectra were referenced to the solvent peak. Melting points (Mp) were recorded using open-end capillaries on a Meltemp melting point apparatus and are uncorrected. Accurate mass measurements were performed either on a Finnigan MAT 8200 mass spectrometer using electronic impact (EI) or chemical ionisation (CI; CH₄) at the University of Western Ontario, or a quadrupole time-of-flight (ES-Q-TOF), model Synapt MS G1 from Waters in positive electrospray mode and spectra were recorded at the Université de Sherbrooke.

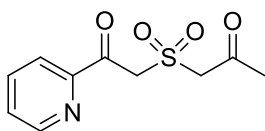
Synthesis of 4:



1-mercapto-propan-2-one (2.42 g, 27 mmol) was dissolved in 300 mL of dry acetonitrile (ACN) at room temperature (RT) and then cooled to 0 °C. Next, 2-bromo-1-(pyridin-2-

yl)ethanone (5.00 g, 27 mmol) was dissolved in 50 mL of ACN and added drop-wise to the former solution over a 30 minute time period. The reaction mixture was allowed to stir for an addition 30 minutes at which point sodium bicarbonate (2.26 g, 27 mmol) was added. The solution was allowed to warm to room temperature and was stirred overnight. The solvent was then removed by rotary evaporation and the brownish oil was added to 200 mL of dichloromethane (DCM) and extracted washed with 3 x 50 mL water, dried over MgSO₄, filtered, and concentrated to a crude yield of 5.02 g. The crude product was then purified by short plug flash column chromatography using 100 mL of DCM:hexanes (8/2) and then flushed with ethyl acetate. Yields range from 92 – 96%. **¹H NMR (400 MHz, CDCl₃, 298 K) δ (ppm) :** 8.66 (d, *J* = 4.7 Hz, 1H), 8.07 (d, *J* = 7.8 Hz, 1H), 7.85 (t, *J* = 7.8 Hz, 1H), 7.51-7.48 (m, 1H), 4.13 (s, 2H). 3.41 (s, 2H), 2.29 (s, 3H); **¹³C NMR (100MHz, CDCl₃, 298 K) δ (ppm) :** 190.1, 183.6, 138.2, 133.7, 128.2, 121.4, 41.8, 39.2, 28.0. **HRMS (EI) *m/z* Calculated :** C₁₀H₁₁NO₂S : 209.0510, **Experimental :** 209.0514. A crystal structure was obtained for this compound.

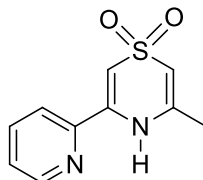
Synthesis of 5:



1-(2-oxo-2-(pyridin-2-yl)ethylthio)propan-2-one **4** (3.63 g, 17 mmol) was dissolved in 100 mL of DCM and cooled to -75 °C using an isopropanol/dry ice bath. To this stirring solution was added 8.55 g of *m*CPBA dissolved in 100 mL of DCM drop-wise over 2 h. The reaction mixture was stirred at -75 °C for an additional 2 h before being allowed to gradually warm overnight. The solution was then neutralized to pH 7 with sodium bicarbonate and extracted 3 times with 75 mL of water. The organic layer was then dried

over MgSO₄, filtered, and concentrated to a crude yield of 3.90 g. The crude sample was then purified by short plug flash column chromatography using Ethyl acetate / DCM (1/1). Yields ranged from 85–94%. **¹H NMR (400 MHz, CDCl₃, 298 K) δ (ppm)** : 8.71 (d, *J* = 4.7 Hz, 1H), 8.08 (d, *J* = 7.8 Hz, 1H), 7.88 (t, *J* = 7.8 Hz, 1H), 7.56-7.52 (m, 1H), 5.21 (s, 2H), 4.45 (s, 2H), 2.40 (s, 3H); **¹³C NMR (100MHz, CDCl₃, 298 K) δ (ppm)** : 197.3, 190.5, 149.3, 137.3, 128.4, 122.6, 63.9, 58.0, 31.9. **HRMS (CI in CH₄) *m/z*** **Calculated** : for [M+H]⁺ C₁₀H₁₂NO₄S : 242.0487, **Experimental** : 242.0480.

Synthesis of 1 (pythdo):



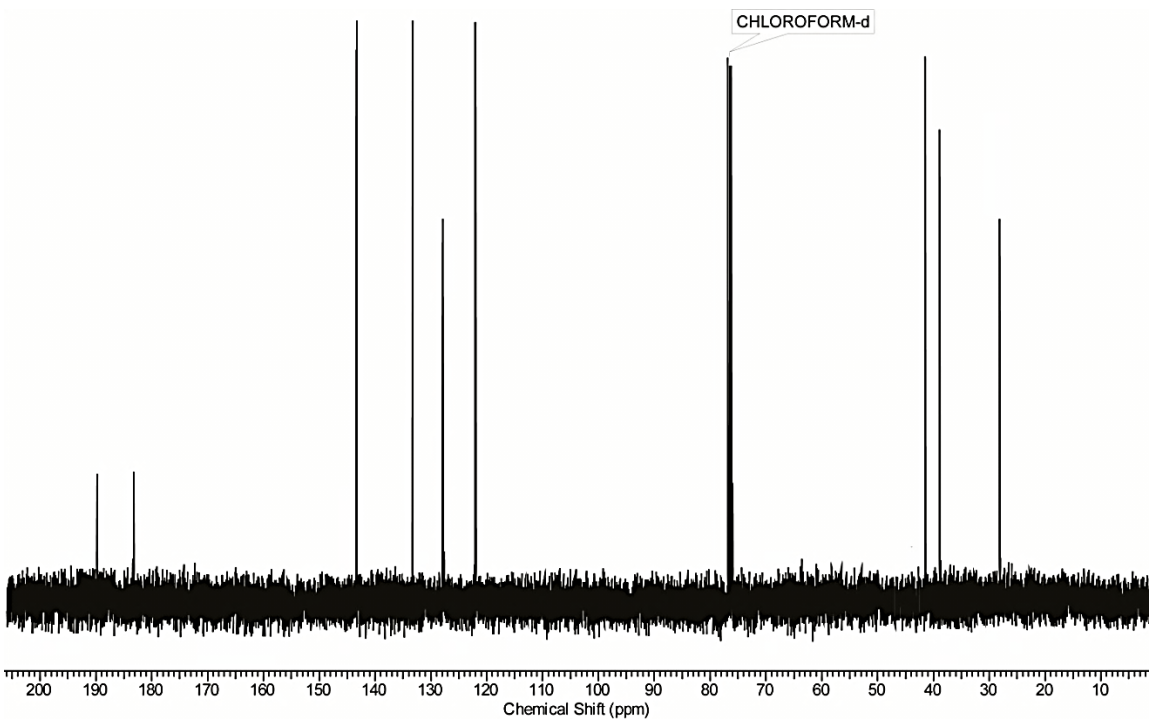
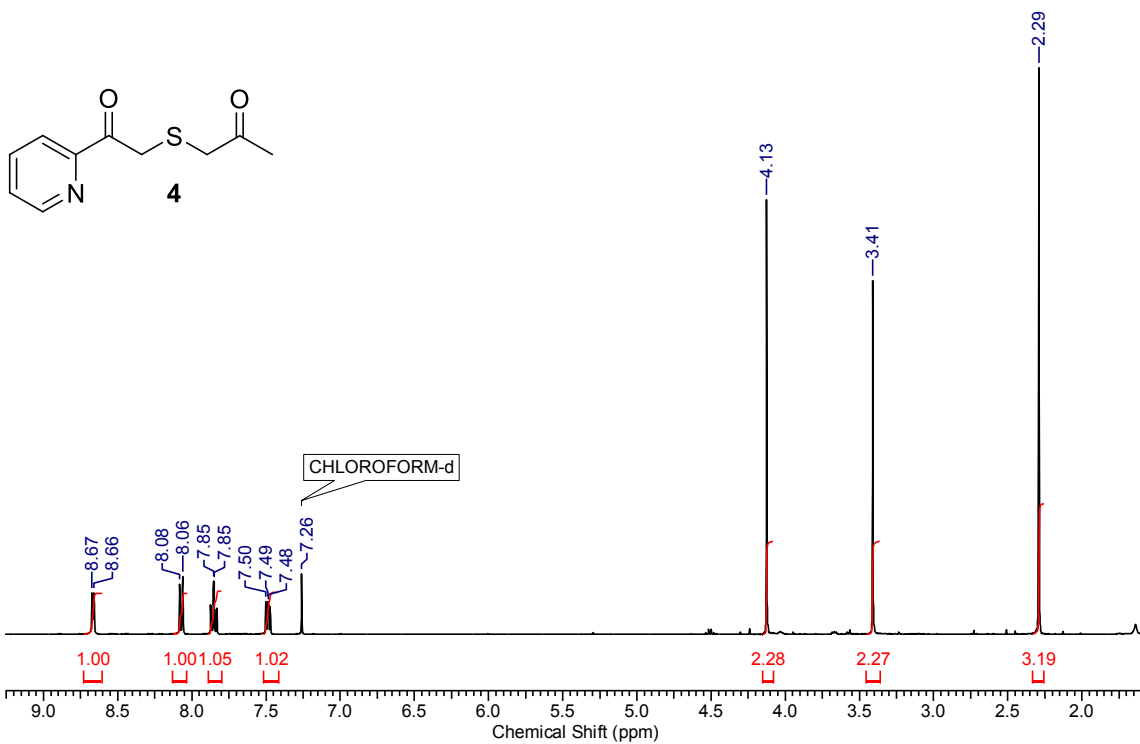
1-(2-oxo-2-(pyridin-2-yl)ethylsulfonyl)propan-2-one **5** (1.22 g, 5.06 mmol) and ammonium acetate (4.4 g, 57 mmol) were dissolved in 40 mL of dimethylformamide (DMF). The reaction mixture was set to reflux for 3 hours and then cooled to room temperature. The solvent was removed *in vacuo* with heating. The crude product was then adsorbed onto minimal silica and purified by flash column chromatography using 75 g of silica and a starting solvent gradient of DCM / Ethyl acetate (9 / 1) with increasing ethyl acetate by 10% every 100 mL. Typical yields were 50 – 63%. **¹H NMR (400 MHz, CDCl₃, 298 K) δ (ppm)** : 9.27 (s, broad, N-H), 8.62 (d, *J* = 4.7 Hz, 1H), 7.87 (dd, *J* = 7.8, 7.8 Hz, 1H), 7.75 (d, *J* = 7.8 Hz, 1H), 7.43 (dd, *J* = 4.7, 7.8 Hz, 1H), 6.51 (d, *J* = 3.9 Hz, 1H), 5.83 (d, *J* = 3.9 Hz, 1H), 2.24 (s, 3H); **¹³C NMR (100MHz, CDCl₃, 298 K) δ (ppm)** : 148.7, 147.0, 141.0, 138.7, 137.8, 125.4, 119.8, 101.5, 99.9, 20.7. **HRMS (EI) *m/z* Calculated** : C₁₀H₁₀N₂O₂S : 222.0463, **Experimental** : 222.0472.

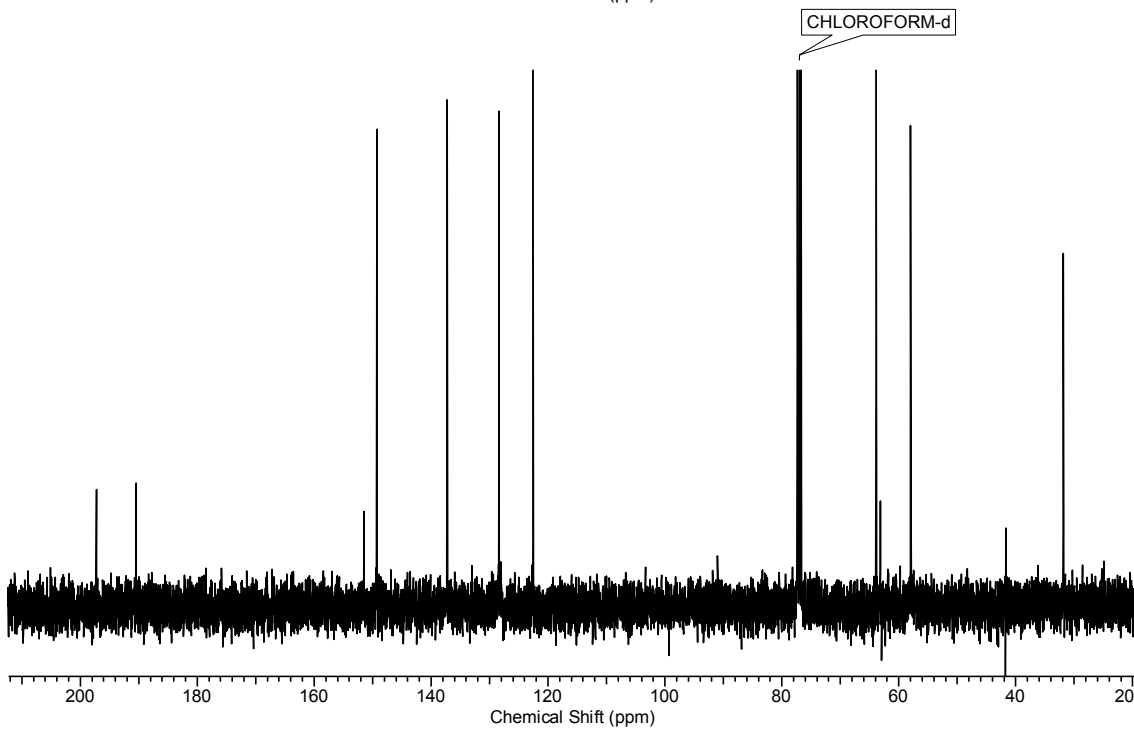
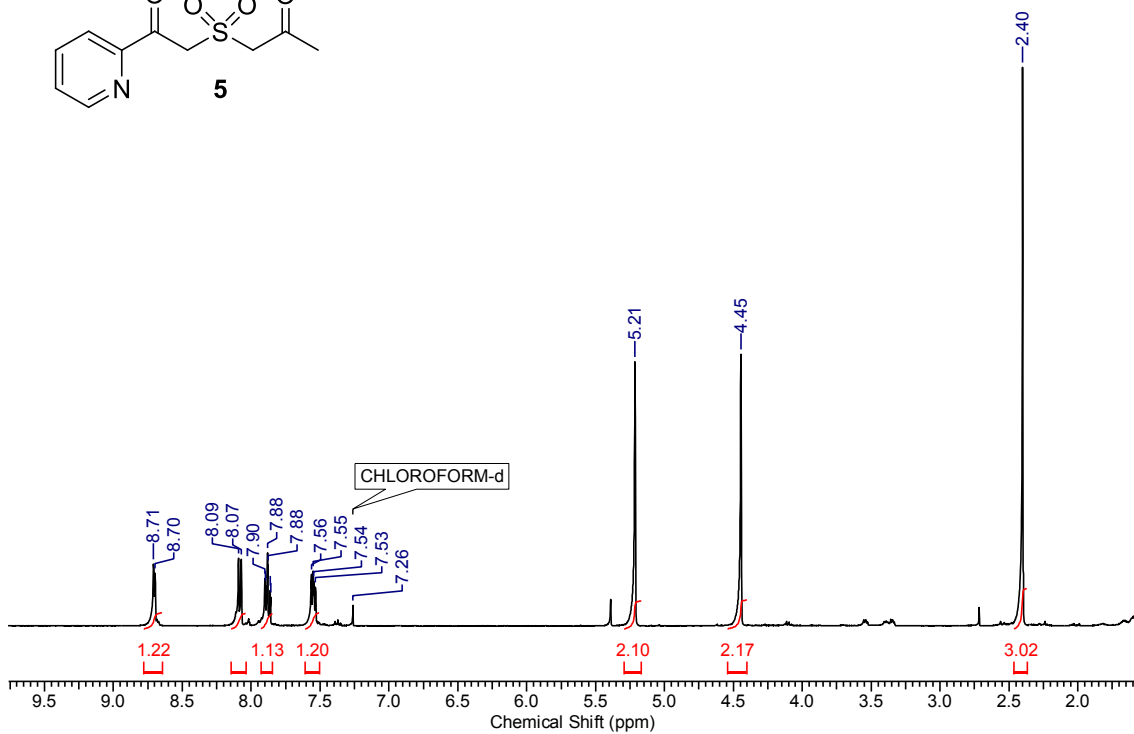
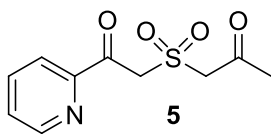
Synthesis of 2 [(ppy)₂Ir(pythdo)]:

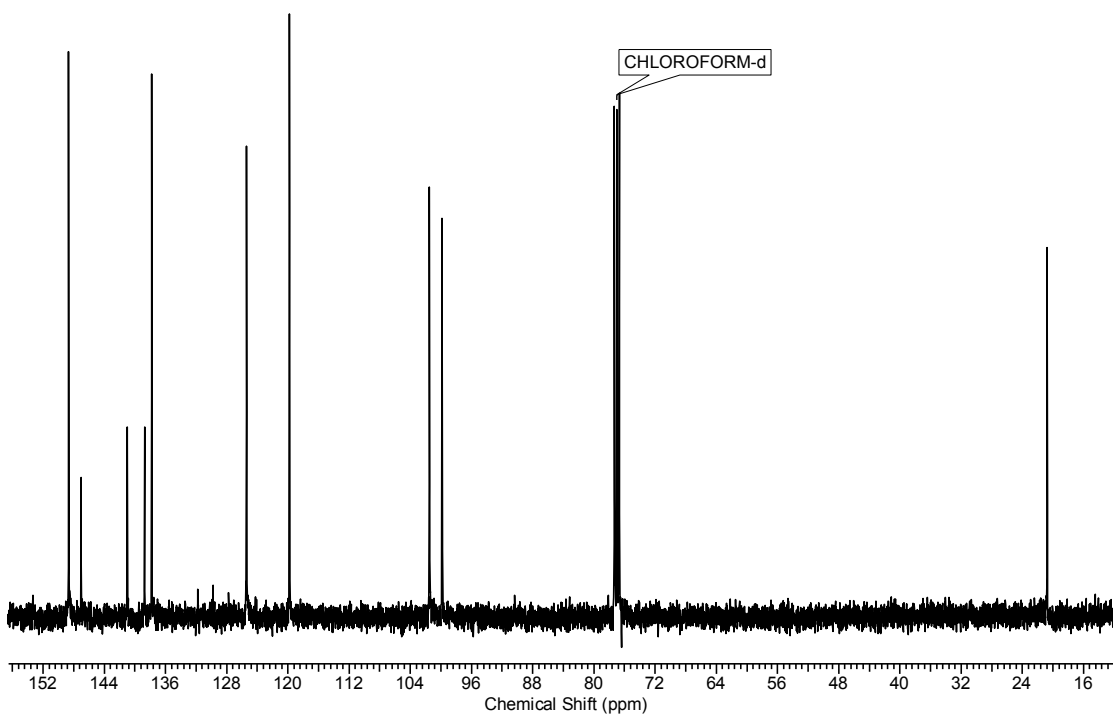
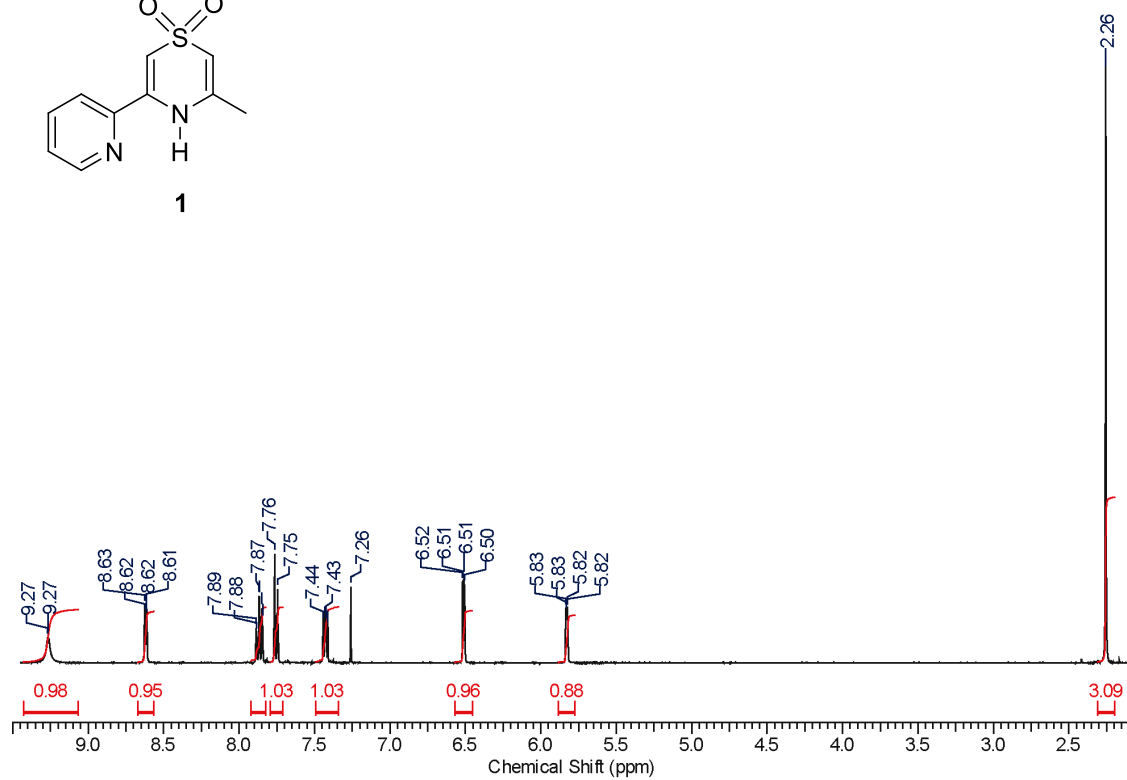
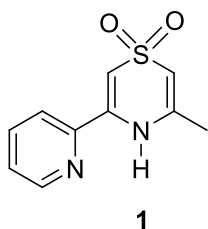
This protocol proceeds via isolation of the μ -dichloro bridged iridium(III) dimer described by Nonoyama.¹ The cleavage of the dimer (393.6 mg, 0.37 mmol, 1.00 equiv.) was accomplished by addition of pythdo (169.8 mg, 0.76 mmol, 2.06 equiv.), potassium carbonate (116.7 mg, 0.84 mmol, 2.28 equiv.) in MeOH and DCM (1/1; 32 mL). The solution was degassed by successive cycles of vacuum and N₂ purging and finally heated at reflux for 18 h. The clear yellow solution was cooled to RT, diluted with water (100 mL) and the resulting aqueous phase was then extracted with DCM. The organic layers were combined, dried over Na₂SO₄, and concentrated to yield a yellow powder that was directly purified by flash chromatography on silica gel using a gradient of DCM and acetone (from 100% DCM to (80/20) DCM/Acetone). A yellow powder was obtained (308.0 mg, 58 %). **R_f**: 0.53 (DCM/MeOH (95/5)). **¹H NMR (400 MHz, CDCl₃) δ (ppm)** : 8.29 (d, J = 5.1 Hz, 1H), 7.97 – 7.89 (m, 2H), 7.85 – 7.67 (m, 5H), 7.59 (dd, J = 7.8, 1.0 Hz, 1H), 7.54 (dd, J = 7.8, 1.1 Hz, 1H), 7.47 (d, J = 5.1 Hz, 1H), 7.17 – 7.09 (m, 2H), 6.97 – 6.90 (m, 2H), 6.87 – 6.78 (m, 2H), 6.71 (td, J = 7.4, 1.3 Hz, 1H), 6.56 (d, J = 4.2 Hz, 1H), 6.13 (dd, J = 7.6, 0.6 Hz, 1H), 6.08 (dd, J = 7.6, 0.6 Hz, 1H), 5.72 (d, J = 4.2 Hz, 1H), 1.38 (s, 3H). **¹³C NMR (101 MHz, CDCl₃) δ (ppm)** : 168.50, 167.70, 160.46, 155.87, 153.38, 151.37, 150.39, 150.36, 149.40, 148.20, 143.52, 142.73, 137.37, 137.27, 137.00, 131.64, 130.84, 130.56, 129.92, 125.45, 124.37, 124.33, 123.03, 122.63, 121.97, 120.93, 119.14, 118.93, 101.14, 99.58, 28.50. **LR-MS (ES-Q-TOF)** : [M+H]⁺: 745.2; [M+Na]⁺: 723.2. **HR-MS (ES-Q-TOF) (C₃₂H₂₆IrN₄O₂S) [M+H]⁺ Calculated** : 723.1406; **Experimental** : 723.1422; **(C₃₂H₂₅IrN₄O₂SNa) [M+Na]⁺ Calculated** :

745.1225; **Experimental** : 745.1216. A crystal structure was obtained for this compound. **Elemental Analysis (C₃₂H₂₅IrN₄O₂S·CH₂Cl₂) Calculated** : C, 49.13; H, 3.37; N, 6.94; **Experimental_{avg}** : C, 49.78; H, 3.40; N, 6.86.

NMR Spectra:







Procedure for UPLC-MS :

Liquid chromatography was run on a BEH C18 column purchased from Waters (2.1 x 100 mm, 1.7 μm) at 0.5 mL/min using an acetonitrile/water (ACN/H₂O) gradient as follows: linear gradient from 2% ACN/H₂O to 98% ACN/H₂O in 6 min; stay still for 1 min; come back to 2% ACN/H₂O in 1 min; equilibrate for 2 min; for a total run time of 10 min. A volume of 3 μL was injected onto the system and the column was kept at 30°C during the analysis. The system used for the analysis was the Nexera instrument (Shimadzu) equipped with a photodiode array detector (Shimadzu) and a mass spectrometer detector (Maxis from Bruker). Recording was done between 190 and 800 nm and between 100 and 1000 amu.

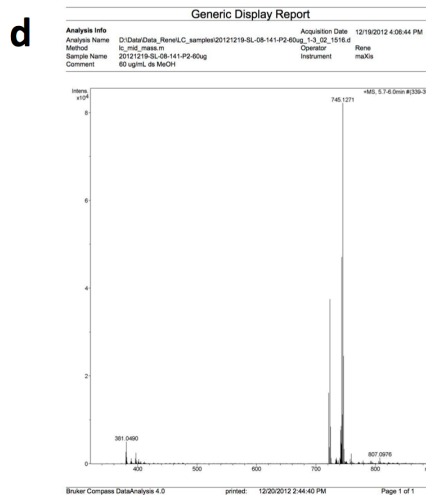
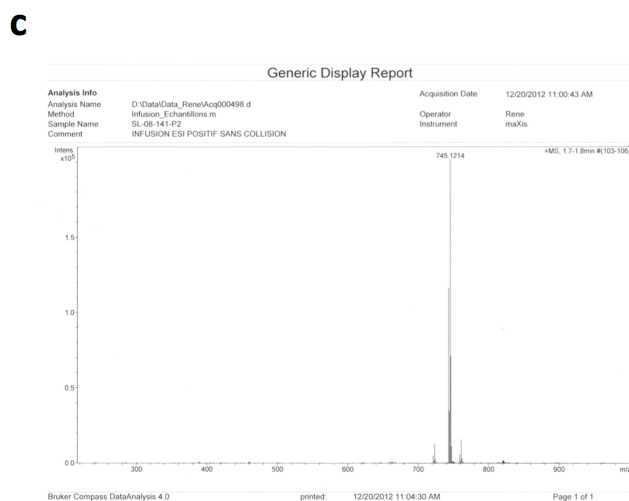
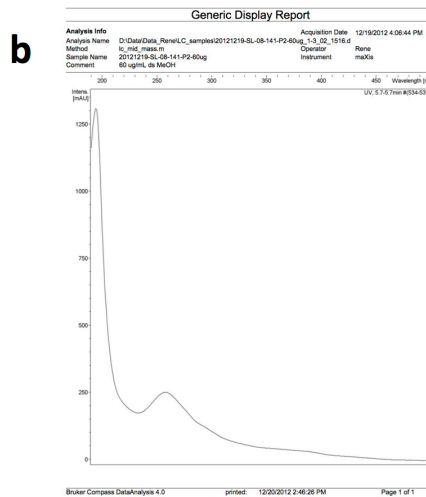
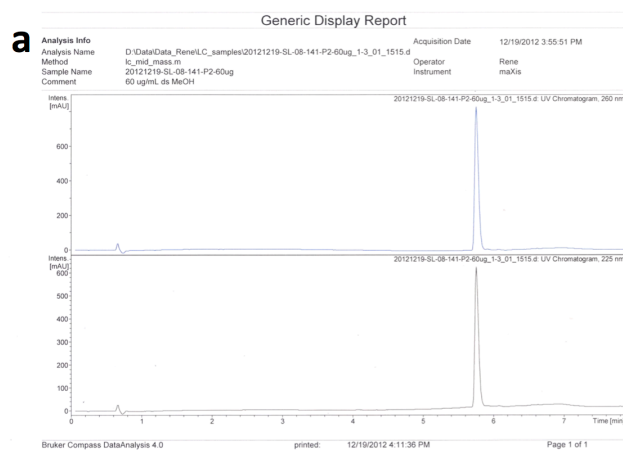


Figure S1 : a) UPLC trace of **2**; b) UV-Vis spectrum of **2** after UPLC; c) ESI-TOF MS of **2** via direct injection into the spectrometer; d) ESI-TOF MS of **2** after UPLC.

General Procedures for X-Ray Crystallography:

The crystals for **1** were grown by slow vapor diffusion of diisopropyl ether into a concentrated chloroform solution while for **2** the same technique was used but with diffusion of diethyl ether in a methanol/ACN solution. A summary of the refinement parameters and the resulting factors is given in Table **S1** and in the following sections. The ORTEP drawings for each at 30% probability are given in Figures **S1**, and **S2**, respectively.

Table S1: Crystallographic Parameters

Compound	1	2
Identification code	b12029_0m	Colman_sl_08_67
Chemical formula	C ₁₀ H ₁₀ N ₂ O ₂ S	C _{32.50} H ₂₇ IrN ₄ O _{2.50} S
Formula weight	222.26	737.84
Temperature	150(2) K	100(2) K
Wavelength	0.71073 Å	1.54178 Å
Crystal size	0.28 x 0.16 x 0.14 mm	0.020 x 0.110 x 0.260 mm
Crystal habit	Clear colorless blocks	clear light yellow Needle
Crystal system	Monoclinic	triclinic
Space group	C2/c	P -1
Unit cell dimensions	a = 10.3350(4) Å α = 90° b = 9.6877(4) Å β = 104.8170(10)° c = 19.17442(9) Å γ = 90°	a = 8.7490(2) Å α = 104.1510(10)° b = 16.2451(4) Å β = 94.4650(10)° c = 21.1497(4) Å γ = 102.1170(10)°
Volume	1911.10(14) Å ³	2823.24(11) Å ³
Z	8	4
Density (calculated)	1.545 mg/cm ³	1.736 Mg/cm ³
Absorption coefficient	0.317 mm ⁻¹	10.167 mm ⁻¹
F(000)	928	1452
Theta range for data collection	2.13 to 28.43°	2.17 to 69.70°
Index ranges	-13<=h<=12, -12<=k<=12, -25<=l<=26	-9<=h<=10, -19<=k<=19, -25<=l<=25
Reflections collected	24310	47407
Independent reflections	2383 [R(int) = 0.0255]	10354 [R(int) = 0.0300]
Coverage of independent reflections	98.9%	97.1%
Absorption correction	Semi-empirical from equivalents	multi-scan
Max. and min. transmission	0.9564 and 0.9156	0.8225 and 0.1774
Structure solution technique	direct methods	direct methods
Structure solution program	SHELXS-97 (Sheldrick, 2008)	SHELXS-97 (Sheldrick, 2008)
Refinement method	Full-matrix least-squares on F ²	Full-matrix least-squares on F ²
Refinement program	SHELXS-97 (Sheldrick, 2008)	SHELXL-97 (Sheldrick, 2008)
Function minimized	Σ w(F _o ² - F _c ²) ²	Σ w(F _o ² - F _c ²) ²
Data / restraints / parameters	2383 / 0 / 137	10354 / 1 / 638
Goodness-of-fit on F ²	1.135	1.266
Δ/σ _{max}		0.058
Final R indices	[I>2σ(I)] R1 = 0.0328, wR2 = 0.1259 all data R1 = 0.0358, wR2 = 0.1296	9518 data; I>2σ(I) R1 = 0.0527, wR2 = 0.1243 all data R1 = 0.0571, wR2 = 0.1288
Weighting scheme	Calc	w=1/[σ ² (F _o ²)+(0.0412P) ² +25.5535P] where P=(F _o ² +2F _c ²)/3
Largest diff. peak and hole	0.492 and -0.274 eÅ ⁻³	3.216 and -3.029 eÅ ⁻³
R.M.S. deviation from mean	0.220 eÅ ⁻³	0.190 eÅ ⁻³

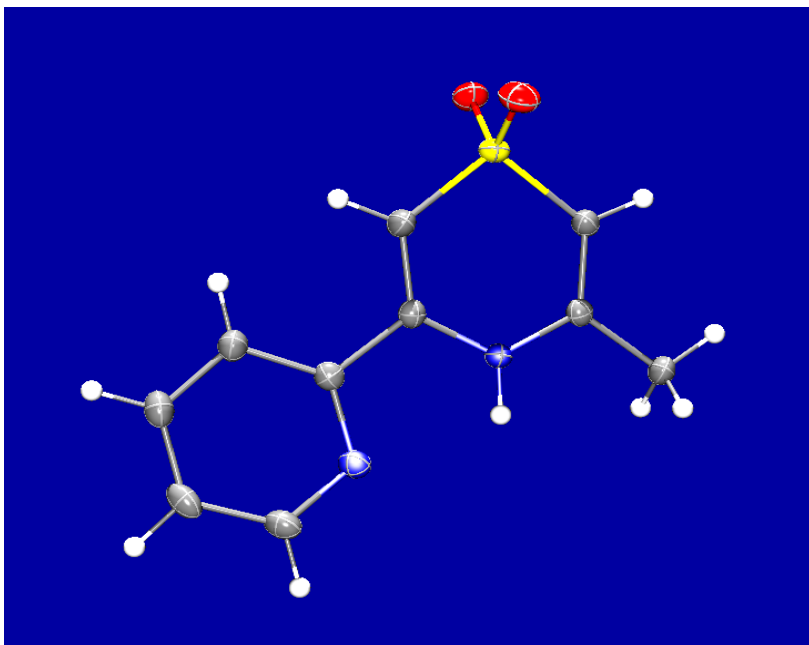


Figure S2: ORTEP representation of **1** at 30% probability.

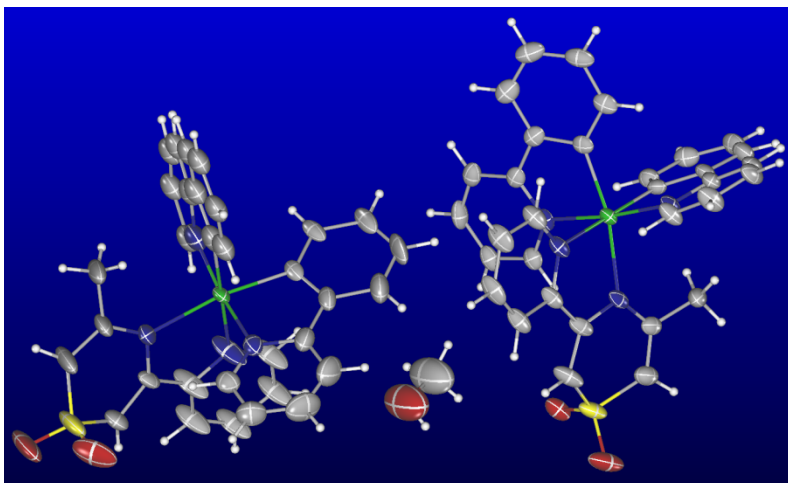


Figure S3: ORTEP representation of **2** at 30% probability.

X-Ray Detailed Procedure for 1:

The X-ray intensity data were measured with a Bruker APEX II diffractometer, a total of 120 frames were collected for a total exposure time of 4.25 hours. The frames were

integrated with the Bruker SAINT software package using a narrow-frame algorithm. The integration of the data using a monoclinic unit cell yielded a total of 24310 reflections to a maximum θ angle of 28.43° , of which 2383 were independent (completeness = 98.9%, $R_{\text{int}} = 2.55\%$ and $R_{\text{sig}} = 2.15\%$). The final cell constants were $a = 10.3350(4) \text{ \AA}$, $b = 9.6877(4) \text{ \AA}$, $c = 19.7442(9) \text{ \AA}$, $\alpha = 90^\circ$, $\beta = 104.8170(10)^\circ$, $\gamma = 90^\circ$, volume = $1911.10(14) \text{ \AA}^3$. Data were corrected for absorption effects using the multi-scan method (SADABS). The calculated minimum and maximum transmission coefficients (based on crystal size) are 0.9156 and 0.9564.

The structure was solved and refined using the Bruker SHELXTL Software Package, using the space group $C2/c$, with $Z = 8$ for the formula unit, $C_{10}H_{10}N_2O_2S$. The final anisotropic full-matrix least-squares refinement on F^2 with 137 variables converged at $R1 = 3.58\%$, for the observed data and $wR2 = 12.96\%$ for all data. The goodness-of-fit was 1.135. The largest peak in the final difference electron density synthesis was $0.492 \text{ e}/\text{\AA}^3$ and the largest hole was $-0.274 \text{ e}/\text{\AA}^3$ with an RMS deviation of $0.220 \text{ e}/\text{\AA}^3$. On the basis of the final model, the calculated density was 1.545 g/cm^3 and $F(000)$, 928 e^- .

X-Ray Detailed Procedure for complex 2:

The X-ray intensity data were measured with a Bruker APEX DUO, a total of 136 frames were collected for a total exposure time of 1.51 hours. The frames were integrated with the Bruker SAINT software package using a narrow-frame algorithm. The integration of the data using a triclinic unit cell yielded a total of 47407 reflections to a maximum θ angle of 69.70° (0.82 \AA resolution), of which 10354 were independent (average

redundancy 4.579, completeness = 97.1%, $R_{\text{int}} = 3.00\%$, $R_{\text{sig}} = 2.43\%$) and 9518 (91.93%) were greater than $2\sigma(F^2)$. The final cell constants of $a = 8.7490(2)$ Å, $b = 16.2451(4)$ Å, $c = 21.1497(4)$ Å, $\alpha = 104.1510(10)^\circ$, $\beta = 94.4650(10)^\circ$, $\gamma = 102.1170(10)^\circ$, volume = $2823.24(11)$ Å³, are based upon the refinement of the XYZ-centroids of 9804 reflections above $20 \sigma(I)$ with $6.231^\circ < 2\theta < 138.2^\circ$. Data were corrected for absorption effects using the multi-scan method (SADABS). The ratio of minimum to maximum apparent transmission was 0.675. The calculated minimum and maximum transmission coefficients (based on crystal size) are 0.1774 and 0.8225.

The structure was solved and refined using the Bruker SHELXTL Software Package, using the space group P -1, with $Z = 4$ for the formula unit, $C_{32.50}H_{27}IrN_4O_{2.50}S$. The final anisotropic full-matrix least-squares refinement on F^2 with 638 variables converged at $R1 = 5.27\%$, for the observed data and $wR2 = 12.88\%$ for all data. The goodness-of-fit was 1.266. The largest peak in the final difference electron density synthesis was $3.216 \text{ e}/\text{Å}^3$ and the largest hole was $-3.029 \text{ e}/\text{Å}^3$ with an RMS deviation of $0.190 \text{ e}/\text{Å}^3$. On the basis of the final model, the calculated density was $1.736 \text{ g}/\text{cm}^3$ and $F(000)$, 1452 e⁻.

General Procedures for Photophysical Characterization:

All samples were prepared in either HPLC or spectroscopic grade solvent with concentrations on the order of $25 \mu\text{M}$. Absorption spectra were recorded at room temperature in a 1.0 cm capped quartz cuvette, using a Shimadzu UV-1800 double beam spectrophotometer. Molar absorptivity determination was verified by linear least squares fit of values obtained from at least three independent solutions at varying concentrations

with absorptions ranging from (0.01-1.6 a.u.). Steady-state emission spectra were obtained by exciting at the longest wavelength absorption maxima using a Horiba Jobin Yvon Fluorolog-3 spectrofluorometer equipped with double monochromators and a photomultiplier tube detector (Hamamatsu model R955). Emission quantum yields were determined using the optically dilute method.² A stock solution for each complex with an absorbance of ca. 0.5 was prepared and then four dilutions were obtained with dilution factors of 40, 20, 13.3 and 10 resulting in optical dilution absorbances of ca. 0.013, 0.025, 0.038 and 0.05, respectively. The Beer-Lambert law was assumed to remain linear at the concentrations of the solutions. The emission spectra were then measured after the solutions were rigorously degassed with solvent-saturated nitrogen gas (N₂) for 20 minutes prior to spectrum acquisition using septa-sealed quartz cells from Starna. For each sample, linearity between absorption and emission intensity was verified through linear regression analysis and additional measurements were acquired until the Pearson regression factor (R²) for the linear fit of the data set surpassed 0.9. Individual relative quantum yield values were calculated for each solution and the values reported represent slope obtained from the linear fit of these results. The equation $\Phi_s = \Phi_r(A_r/A_s)(I_s/I_r)(n_s/n_r)^2$ was used to calculate the relative quantum yield of the sample, where Φ_r is the absolute quantum yield of the reference, n is the refractive index of the solvent, A is the absorbance at the excitation wavelength, and I is the integrated area under the corrected emission curve. The subscripts s and r refer to the sample and reference, respectively. For the phosphorescent samples, a solution of [Ru(bpy)₃](PF₆)₂ in ACN ($\Phi_r = 0.095$)³ was used as the external reference, while to determine fluorescence quantum yield Quinine bisulfate in 0.1N HCl ($\Phi_r = 0.54$).⁴ The experimental uncertainty in the emission quantum

yields is conservatively estimated to be 10%, though we have found that statistically we can reproduce PLQYs to 3% relative error. Absolute quantum yield method was used to determine the quantum yield of solid sample (thin films and powder) using a Hamamatsu Photonics absolute PL quantum yield measurement system (C9920-02) equipped with a L9799-01 CW xenon light source (150 W), monochromator, C7473 photonic multichannel analyzer, and integrating sphere and employing U6039-05 PLQY measurement software (Hamamatsu Photonics, Ltd., Shizuoka, Japan)

Time-resolved excited-state lifetime measurements were determined using the time-correlated single photon counting (TCSPC) option of the Jobin Yvon Fluorolog-3 spectrofluorometer. A pulsed NanoLED at 341 nm, (pulse duration < 1 ns; fwhm = 14 nm), mounted directly on the sample chamber at 90° to the emission monochromator, was used to excite the samples and photons were collected using a FluoroHub single-photon-counting detector from Horiba Jobin Yvon. The luminescence lifetimes were obtained using the commercially available Horiba Jobin Yvon Decay Analysis Software version 6.4.1, included within the spectrofluorometer. Lifetimes were determined through an assessment of the goodness of its mono exponential fit by minimizing the chi-squared function (χ^2) and by visual inspection of the weighted residuals.

Miscellaneous Photophysical Measurements:

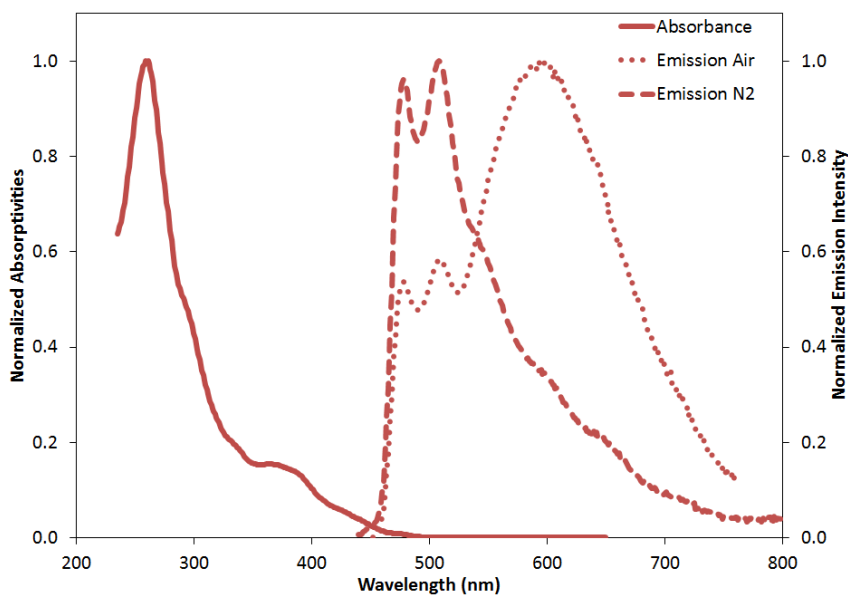


Figure S4 : Absorption spectra (solid line), deaerated (dashed line) and aerated (dotted line) 298 K emission spectra respectively of [Ir(ppy)₂(pythdo)] (2) in ACN.

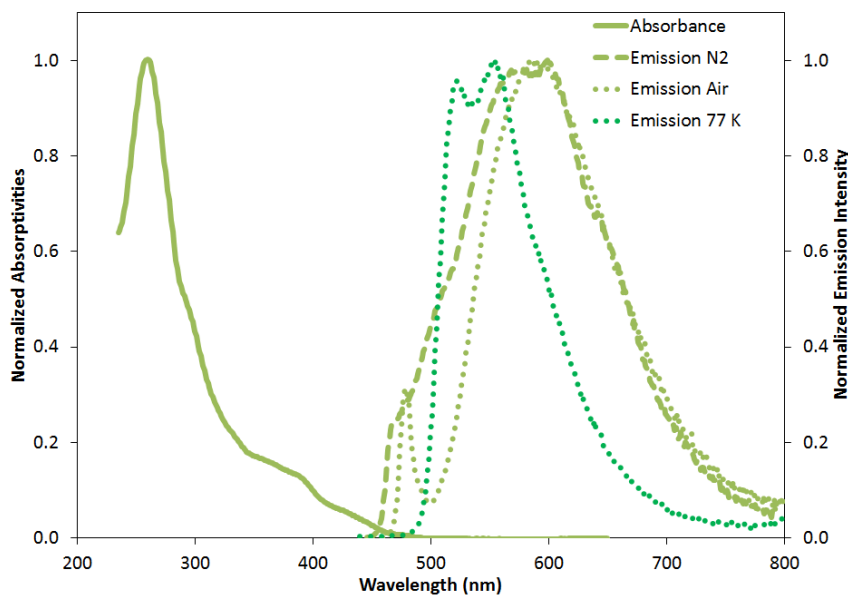


Figure S5 : Absorption spectra (solid line), deaerated (dashed line), aerated (dotted line) 298 K and 77 K (dark green dotted line) emission spectra respectively of [Ir(ppy)₂(pythdo)] (2) in MeOH/EtOH (1/1).

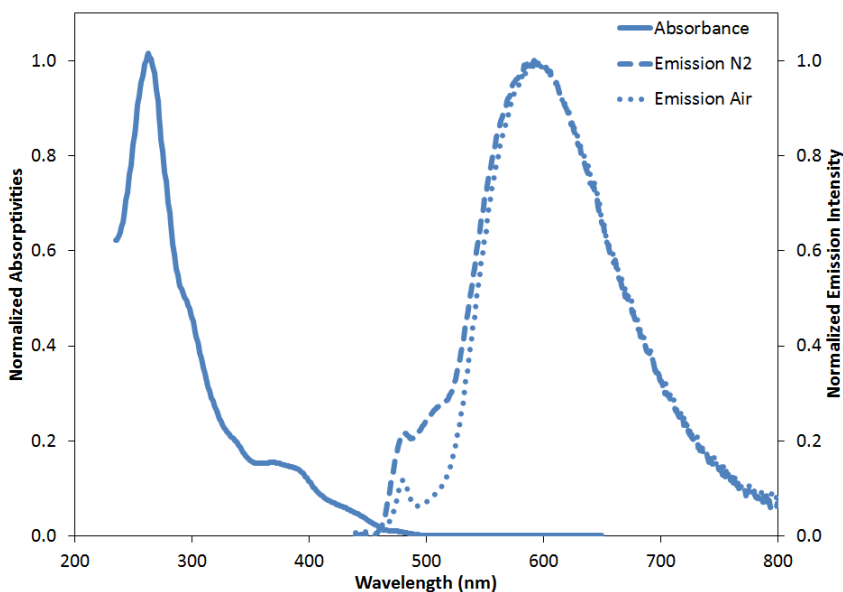


Figure S6 : Absorption spectra (solid line), deaerated (dashed line) and aerated (dotted line) 298 K emission spectra respectively of $[\text{Ir}(\text{ppy})_2(\text{pythdo})]$ (**2**) in DCM.

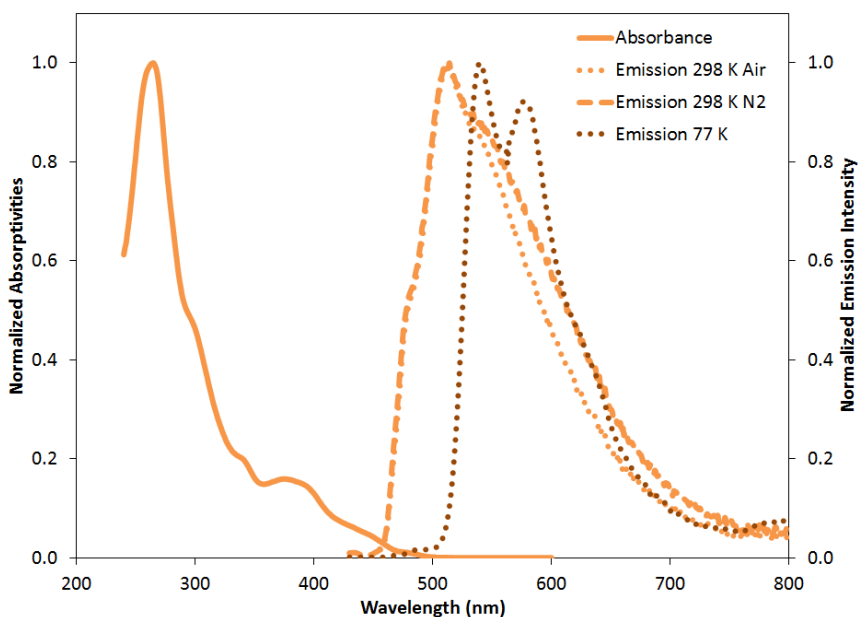


Figure S7: Absorption spectra (solid line, orange), deaerated (dashed line, orange), aerated (dotted line orange) 298 K and 77K (dashed line, brown) emission spectra respectively of $[\text{Ir}(\text{ppy})_2(\text{pythdo})]$ (**2**) in 2-MeTHF.

Table S2: Photophysical properties of complex **2** in deaerated 2-MeTHF solutions.

Emission		τ_e	
77 K (nm) ^a	298 K (nm) ^a	77 K (μ s)	298 K (ns)
470 [0.006]	514 [1.00]	-	1.72×10^3 [84%]
485 [0.016]		-	925 [16%]
540 [1.00]		2.83 [28%]	-
		8.60 [72%]	
576 [0.92]		-	-
600 [0.65]	600 [0.57]	1.97 [18%]	820 [35%]
		8.12 [82%]	1.16×10^3 [65%]

^a Values in brackets refer to the relative intensity of the emission to λ_{\max} .

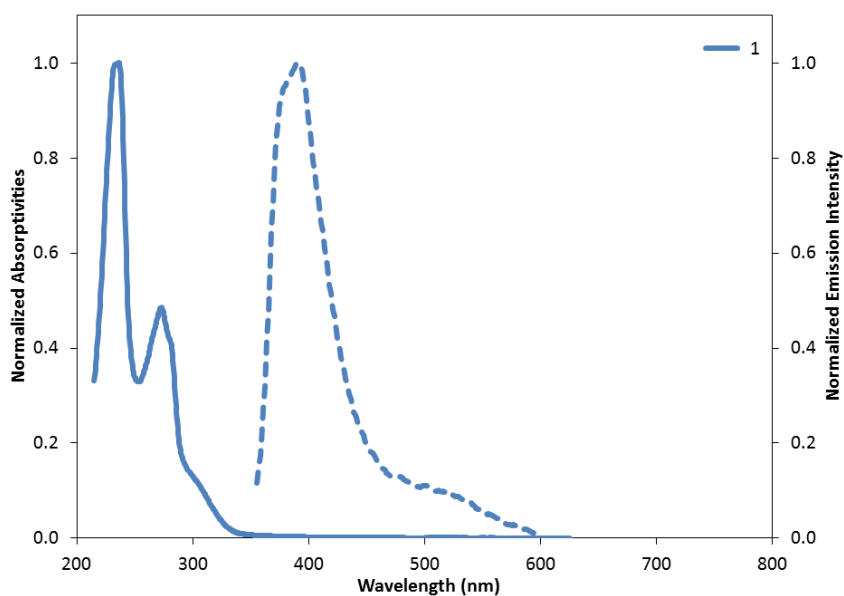


Figure S8 : Absorption spectra (ACN; solid line), 298 K emission (ACN; dashed line) spectra respectively of pythdo ligand.

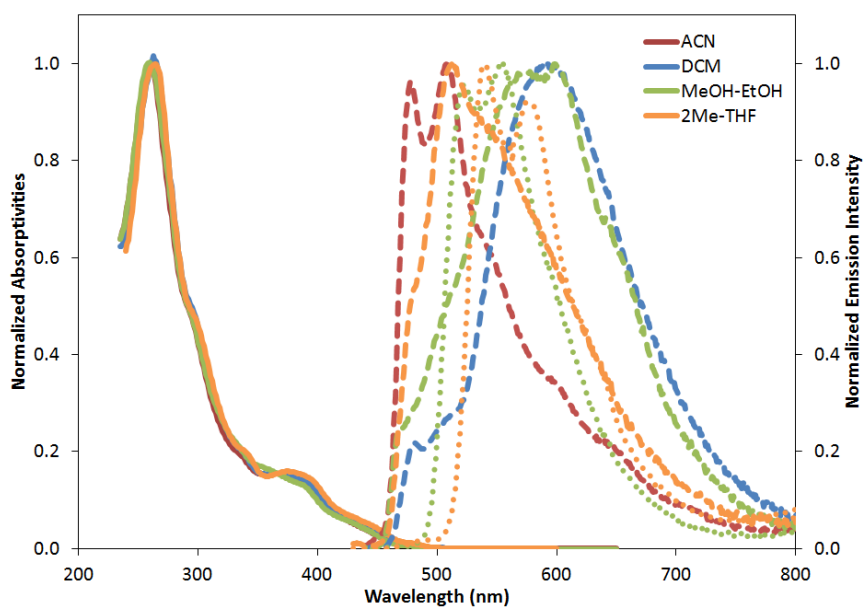


Figure S9 : Solvent study, ACN (red), DCM (blue), 2-MeTHF (orange) and MeOH/EtOH (1/1) (green) on photophysical properties. Absorption spectra (solid line), 298 K deaerated emission (dashed line) and 77 K emission (dotted line) spectra, respectively, of $[\text{Ir}(\text{ppy})_2(\text{pythdo})]$ (**2**).

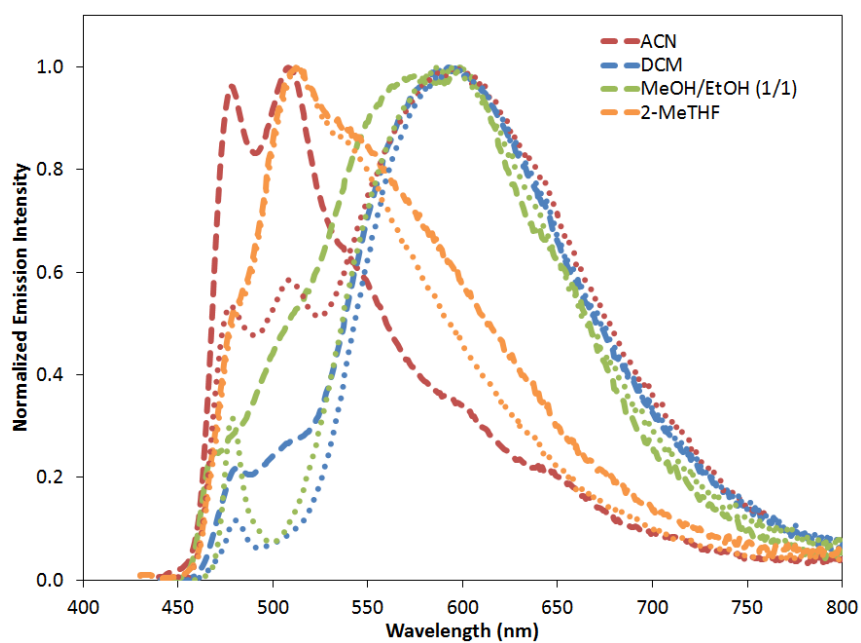
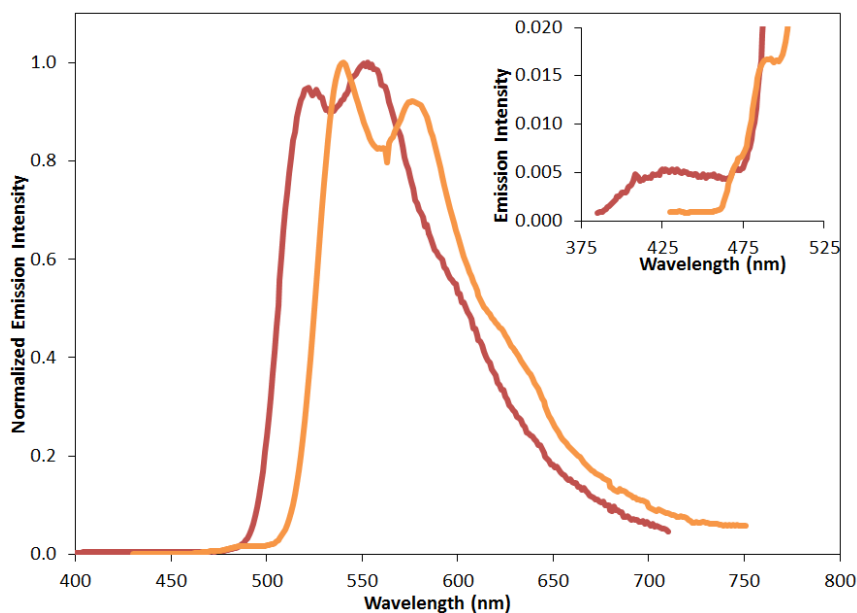


Figure S10 : Solvent study, ACN (red), DCM (blue), 2-MeTHF (orange) and MeOH/EtOH (1/1) (green) on 298 K deaerated emission (dashed line) and aerated emission (dotted line) spectra, respectively, of $[\text{Ir}(\text{ppy})_2(\text{pythdo})]$ (**2**).



Figures S11: 77 K MeOH/EtOH (1/1) (red) and 2-MeTHF (orange) emission spectra of **2**. Inset: Magnification of the previous spectra.

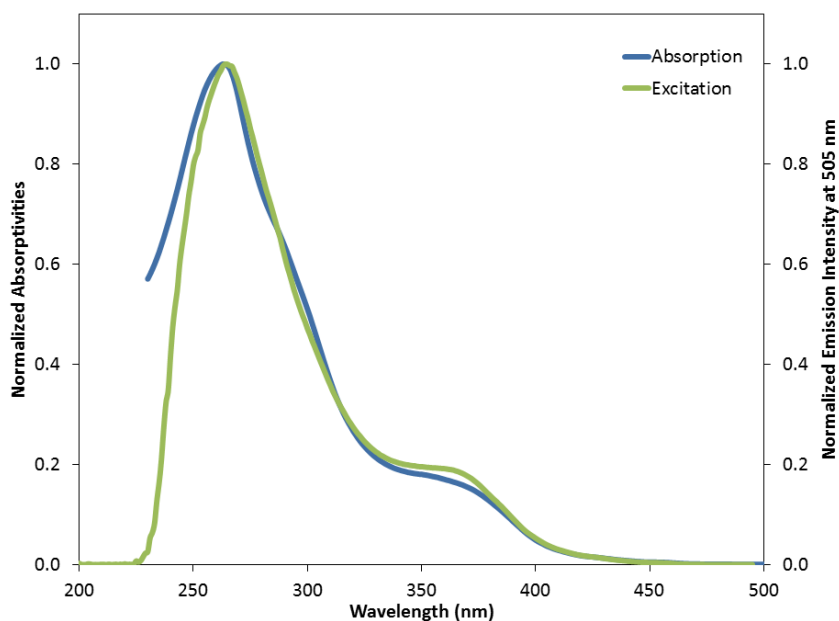


Figure S12 : Absorption spectrum (blue) and excitation spectrum (green) acquired at 505 nm of [Ir(ppy)₂(pythdo)] (**2**) in ACN.

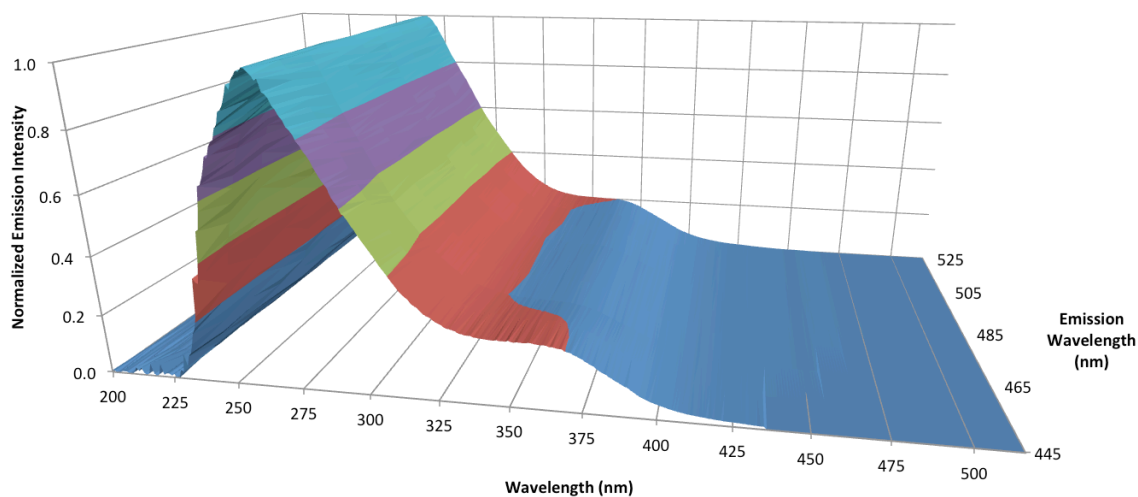


Figure S13 : Normalized excitation spectra acquired at various emission wavelength (445; 455; 465; 475; 485; 495; 505; 515 and 525 nm) of [Ir(ppy)₂(pythdo)] (**2**) in ACN.

Table S3: Estimated Quantum Yields of isoabsorbing solutions (λ_{ex} : 390 nm) of **2**.

Solvent	Integrated Emission	Normalized Integration	Estimated QY (%) ^a
ACN (N ₂)	230629226	1	(1.8) ^b
ACN (Air)	39013833.25	0.17	0.30
MeOH/EtOH (N ₂)	49204046.61	0.21	0.37
DCM (N ₂)	83269350.71	0.36	0.65

^a Calculated relative to the photoluminescent quantum yield (PLQY) measured in ACN under nitrogen. ^b Experimentally determined PLQY.

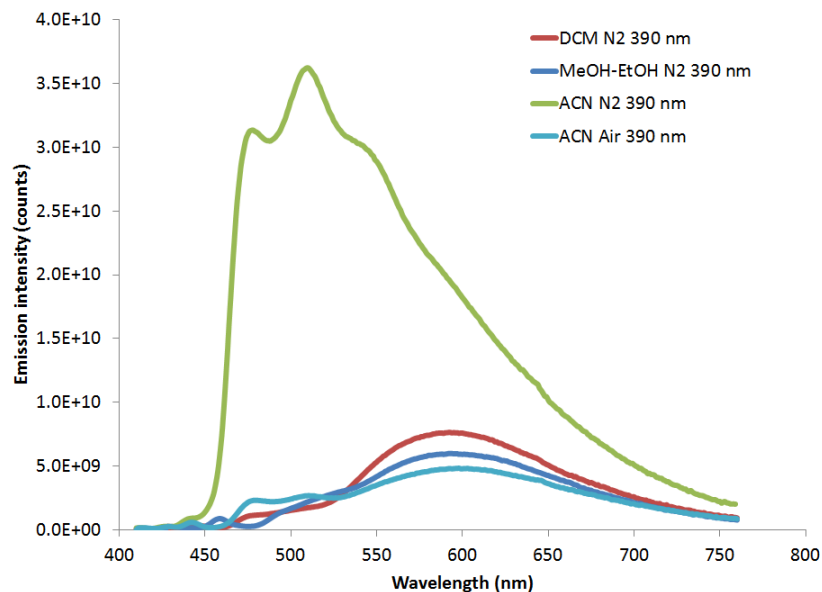


Figure S14: Emission spectra of isoabsorbing solutions ($\lambda_{\text{ex}} = 390 \text{ nm}$) of **2** in DCM (red), MeOH/EtOH (dark blue), ACN (green), aerated ACN (light blue).

Procedure for Measurement of O₂ Quenching:

In addition to the detailed procedure previously outlined in the “**General Procedures for Photophysical Characterization**” section, the sample were degassed for 10 min with the appropriate gas by bubbling the solvent saturated gas directly inside the solution, using a septum sealed cuvette. These gases (20% O₂/80% N₂, 50% O₂/50% N₂, 100% O₂) were directly purchased from Praxair Canada. The same solution of **2** was used for all measurements and between each measurement, the solution was saturated with the 100% N₂ gas and emission was measured to ensure the reproducibility of the measurements. The Stern-Volmer (K_{SV}) constant and the bimolecular quenching constant (k_q) were calculated according to Equations (1) and (2):

$$(1) \quad \frac{I_0}{I} = 1 + K_{\text{SV}}[O_2]$$

$$(2) \quad \frac{I_0}{I} = 1 + \tau_0 k_q [O_2]$$

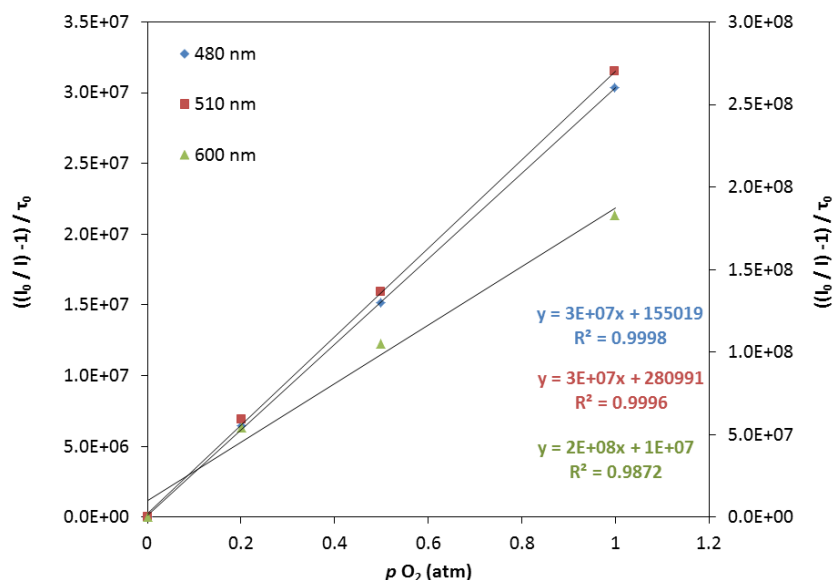


Figure S15: Determination of the Stern-Volmer parameters. Right scale is for data taken at 480 and 510 nm while the left scale is for data measured at 600 nm.

General Procedures for Electrochemical Characterization :

Cyclic voltammetry measurements were performed on an Electrochemical Analyzer potentiostat model 600D from CH Instruments. Solutions for cyclic voltammetry were prepared in ACN and degassed with ACN-saturated nitrogen bubbling for ca. 15 min prior to scanning. Tetra(*n*-butyl)ammoniumhexafluorophosphate (TBAPF₆; ca. 0.1 M in ACN) was used as the supporting electrolyte. It was recrystallized twice from EtOH and dried under vacuum prior to use. A non-aqueous Ag/Ag⁺ electrode (silver wire in a solution of 0.1 M AgNO₃ in ACN) was used as the pseudoreference electrode; a glassy-carbon electrode was used for the working electrode and a Pt electrode was used as the counter electrode. The redox potentials are reported relative to a saturated calomel (SCE)

electrode with a ferrocenium/ferrocene (Fc^+/Fc) redox couple as an internal reference (0.40 V vs SCE).⁵

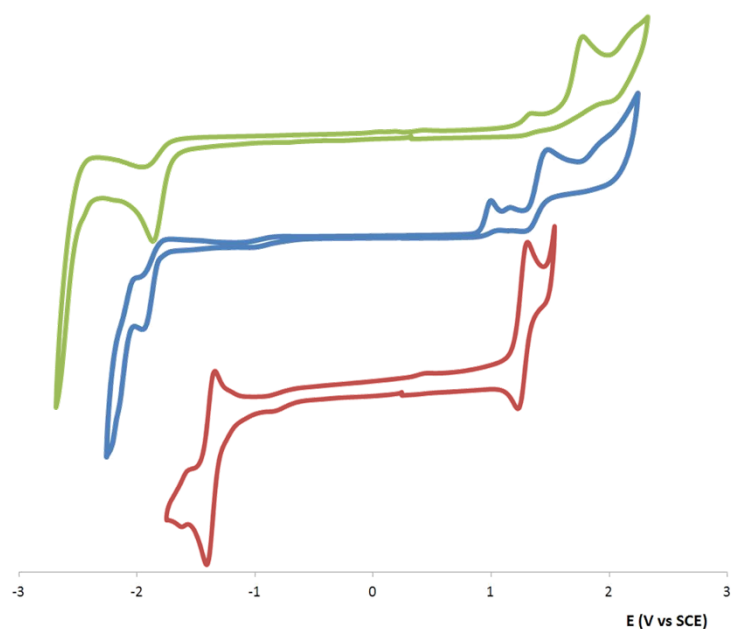


Figure S16: Cyclic voltammograms of pythdo (**1**) (green), $[\text{Ir}(\text{ppy})_2(\text{pythdo})]$ (**2**) (blue) and $[\text{Ir}(\text{ppy})_2(\text{bpy})]\text{PF}_6$ (**3**) (red) in ACN with 0.1 M NBu_4PF_6 ; potentials vs SCE.

General Procedures for Thin Film Measurements:

Stock solutions of **2** (7.64 mg, in 2.5 mL of ACN, 4.32×10^{-3} M) and PMMA (40.7 mg, in 4.0 mL of ACN) were obtained after stirring overnight or until complete dissolution was observed. Different volumes of these stock solutions were combined according to Table S4 and stored in glass vials and were homogenized by manual agitation. The final solutions were spin coated on a quartz substrate and heated at ca. 100°C for 15 min to remove excess of solvent. The quartz substrates were maintained in the excitation beam by a home-made holder and the emission signal was acquired as usual.

Table S4: Preparation of PMMA doped films

Amount of complex (μL)	800	165	215
Calculate weight of complex (mg)	2.44	0.50	0.66
Amount of PMMA (μL)	25	25	50
Calculate weight of PMMA (mg)	0.25	0.25	0.51
% (w/w) of PMMA	90	50	33

Calculation Methodology:

Density Functional Theory (DFT) Calculations. Calculations were performed with Gaussian 09⁶ at the Université de Sherbrooke with Mammouth super computer supported by le Réseau Québécois de Calculs de Haute Performances and Compute Canada. The X-Ray structure was used as the input geometry for the S_0 optimization calculation. The DFT⁷ and TD-DFT⁸ were calculated with the B3LYP method; excited-state triplet geometries were calculated using the unrestricted B3LYP method (UB3LYP).⁹ The 6-31G* basis set¹⁰ was used for C, H and N directly linked to the Iridium atom while the other C, H, N and F atoms were undertaken with the 3-21G* basis set,¹¹ and the VDZ (valence double ζ) with SBKJC effective core potential basis set^{11a, 12} was used for Iridium. The predicted phosphorescence wavelengths were obtained by energy differences between the Triplet and Singlet optimized states.¹³ The energy, oscillator strength and related MO contributions for the 100 lowest singlet-singlet and 5 lowest singlet-triplet excitations were obtained from the TD-DFT/Singlets and the TD-DFT/Triplets output files, respectively. The calculated absorption spectra were visualized with GaussSum 2.1 (fwhm: 1000 cm^{-1}).¹⁴ All calculations were performed in acetonitrile solution through use of the polarized continuum (PCM) solvation model as implemented in Gaussian 09.¹⁵

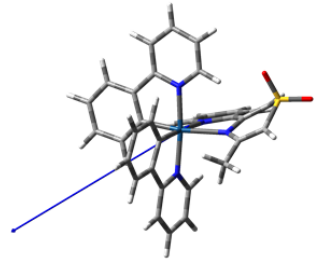
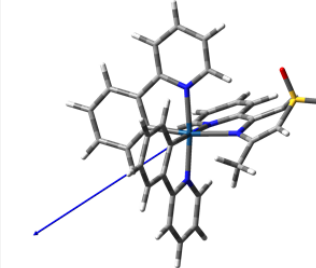
	Singlet State (S_0)	Triplet State (T_1)
		
Scaling Factor	1	1
Magnitude of dipole (D)	14.0121	9.2997

Figure S17: Visualization and magnitude of the dipole moment in the singlet and triplet state.

Table S5: Quantification of the molecular orbital coefficients of **2**^a.

Orbitals Energy (eV)	Molecular sections	Contribution (%)	Visualization	Orbitals Energy (eV)	Molecular sections	Contribution (%)	Visualization
LUMO -1.74	Ir	1.9%		HOMO -5.42	Ir	31.2%	
	ppy	28.0%			ppy	17.6%	
	pythdo	70.1%			pythdo	51.2%	
LUMO+1 -1.63	Ir	3.4%		HOMO-1 -5.6	Ir	34.1%	
	ppy	73.8%			ppy	35.0%	
	pythdo	22.8%			pythdo	30.8%	
LUMO+2 -1.5	Ir	4.9%		HOMO-2 -6.19	Ir	21.2%	
	ppy	85.4%			ppy	73.3%	
	pythdo	9.7%			pythdo	5.5%	
LUMO+3 -1.23	Ir	3.6%		HOMO-3 -6.27	Ir	54.2%	
	ppy	27.0%			ppy	37.2%	
	pythdo	69.4%			pythdo	8.6%	
LUMO+4 -1.02	Ir	7.3%		HOMO-4 -6.52	Ir	34.1%	
	ppy	70.2%			ppy	41.0%	
	pythdo	22.5%			pythdo	25.0%	

^a The different categories indicate the total of orbital contributions (in %) situated on atom(s) composing the metal center, the cyclometallating ligands (ppy) and the ancillary ligand (pythdo).

Table S6: Energy and composition of TD-DFT calculated singlet-singlet transitions of 2
 [Ir(ppy)₂(pythdo)]:

No.	Energy (cm ⁻¹)	Wavelength (nm)	Oscillator Strength	Symmetry	Major contributions
1	24265.4	412.1	0.0337	Singlet-A	HOMO->LUMO (77%), HOMO->L+1 (12%)
2	24774.3	403.6	0.0338	Singlet-A	HOMO->LUMO (17%), HOMO->L+1 (71%)
3	25851.9	386.8	0.0389	Singlet-A	HOMO->L+2 (84%)
4	25932.5	385.6	0.0385	Singlet-A	H-1->LUMO (86%)
5	26761.7	373.7	0.0374	Singlet-A	H-1->L+1 (81%), HOMO->L+1 (10%)
6	27632.7	361.9	0.0292	Singlet-A	H-1->L+2 (84%)
7	28532.1	350.5	0.0103	Singlet-A	HOMO->L+3 (96%)
8	30031.5	333.0	0.0311	Singlet-A	H-1->L+3 (57%), HOMO->L+4 (38%)
9	30108.9	332.1	0.0817	Singlet-A	H-3->LUMO (36%), H-2->LUMO (38%)
10	30419.4	328.7	0.0353	Singlet-A	H-1->L+3 (35%), HOMO->L+4 (47%) H-3->L+1 (38%), H-2->L+1 (30%), HOMO->L+5 (11%)
11	30623.5	326.5	0.0866	Singlet-A	HOMO->L+5 (81%)
12	30791.2	324.8	0.0199	Singlet-A	H-3->LUMO (41%), H-2->LUMO (40%)
13	31361.5	318.9	0.0298	Singlet-A	H-3->L+1 (14%), H-1->L+4 (59%)
14	31755.9	314.9	0.0405	Singlet-A	
15	32101.9	311.5	0.0146	Singlet-A	H-3->L+1 (25%), H-2->L+1 (38%), H-1->L+4 (20%)
16	32197.1	310.6	0.0171	Singlet-A	H-3->L+2 (24%), H-2->L+2 (43%), H-1->L+4 (10%)
17	32295.5	309.6	0.0045	Singlet-A	H-1->L+5 (79%)
18	32890.7	304.0	0.1244	Singlet-A	H-3->L+2 (52%), H-2->L+2 (24%)
19	33102.0	302.1	0.0081	Singlet-A	H-4->LUMO (69%)
20	34136.8	292.9	0.0066	Singlet-A	H-5->L+1 (11%), H-4->L+1 (60%)
21	34326.4	291.3	0.0600	Singlet-A	H-3->L+3 (33%), H-2->L+3 (32%)
22	34649.8	288.6	0.0012	Singlet-A	H-5->LUMO (70%)
23	34675.6	288.4	0.1096	Singlet-A	H-5->L+2 (13%), H-4->L+2 (63%) H-6->L+1 (10%), H-5->L+1 (25%), H-4->L+1 (10%), H- 2->L+3 (17%)
24	35121.7	284.7	0.1517	Singlet-A	H-6->LUMO (64%)
25	35462.0	282.0	0.1316	Singlet-A	H-5->L+1 (41%), H-3->L+3 (23%)
26	35604.8	280.9	0.2604	Singlet-A	H-7->LUMO (39%), H-3->L+3 (11%), H-2->L+3 (25%)
27	35808.8	279.3	0.0471	Singlet-A	H-7->LUMO (23%), H-6->L+1 (17%), H-3->L+4 (24%)
28	36128.2	276.8	0.0776	Singlet-A	
29	36196.0	276.3	0.0543	Singlet-A	H-5->L+2 (35%), H-2->L+3 (10%), H-2->L+4 (21%)
30	36284.7	275.6	0.0028	Singlet-A	H-6->L+1 (37%), H-5->L+2 (10%), H-2->L+4 (20%)
31	36544.4	273.6	0.0681	Singlet-A	H-7->L+1 (63%), H-5->L+2 (10%) H-7->L+2 (18%), H-6->L+1 (12%), H-6->L+2 (20%), H- 2->L+5 (13%)
32	36821.9	271.6	0.0752	Singlet-A	HOMO->L+6 (15%), HOMO->L+9 (21%)
33	37110.6	269.5	0.0772	Singlet-A	H-6->L+2 (47%), H-3->L+5 (11%)
34	37322.8	267.9	0.1980	Singlet-A	H-4->L+3 (33%)
35	37467.1	266.9	0.0312	Singlet-A	
36	37597.8	266.0	0.0683	Singlet-A	H-7->L+2 (14%), H-4->L+3 (38%), H-3->L+4 (13%) H-7->L+2 (21%), H-6->L+2 (12%), H-3->L+5 (40%), H- 2->L+4 (10%)
37	37746.2	264.9	0.0928	Singlet-A	
38	37859.1	264.1	0.2480	Singlet-A	H-7->L+2 (17%), H-3->L+5 (21%), H-2->L+5 (46%)
39	38500.3	259.7	0.1959	Singlet-A	H-1->L+7 (14%), HOMO->L+7 (34%)
40	38793.1	257.8	0.0212	Singlet-A	H-5->L+3 (63%), H-4->L+3 (11%) H-5->L+3 (16%), H-1->L+6 (16%), H-1->L+9 (16%), HOMO->L+6 (21%)
41	39184.3	255.2	0.0759	Singlet-A	H-4->L+4 (53%)
42	39324.6	254.3	0.1613	Singlet-A	H-4->L+4 (16%), H-1->L+9 (16%), HOMO->L+6 (17%), HOMO->L+7 (14%)
43	39389.2	253.9	0.0301	Singlet-A	
44	39677.9	252.0	0.0184	Singlet-A	H-7->L+3 (11%), H-6->L+3 (42%), H-4->L+5 (21%)
45	39689.2	252.0	0.0094	Singlet-A	H-6->L+3 (17%), H-5->L+5 (10%), H-4->L+5 (55%)
46	39973.9	250.2	0.0044	Singlet-A	H-8->LUMO (81%)
47	40069.9	249.6	0.0024	Singlet-A	H-7->L+3 (72%), H-6->L+3 (12%) H-3->L+9 (12%), H-1->L+6 (12%), H-1->L+7 (13%), HOMO->L+7 (16%)
48	40357.0	247.8	0.0838	Singlet-A	H-8->L+1 (31%), H-5->L+4 (35%)
49	40539.3	246.7	0.0096	Singlet-A	H-8->L+1 (23%), H-5->L+4 (46%)
50	40671.6	245.9	0.0360	Singlet-A	

No.	Energy (cm ⁻¹)	Wavelength (nm)	Oscillator Strength	Symmetry	Major contributions
51	40974.1	244.1	0.0025	Singlet-A	H-9->LUMO (62%)
52	40982.9	244.0	0.0086	Singlet-A	H-5->L+5 (63%), H-4->L+5 (12%)
53	41160.4	243.0	0.0557	Singlet-A	H-3->L+9 (10%), H-1->L+7 (36%)
54	41262.8	242.3	0.0488	Singlet-A	H-5->L+5 (10%), H-3->L+9 (14%), H-1->L+6 (15%), H-1->L+9 (13%)
55	41393.5	241.6	0.0033	Singlet-A	H-6->L+4 (68%)
56	41455.6	241.2	0.0076	Singlet-A	H-11->LUMO (22%), H-8->L+2 (16%)
57	41574.9	240.5	0.0141	Singlet-A	H-7->L+4 (35%), H-6->L+5 (17%), HOMO->L+8 (16%)
58	41770.9	239.4	0.0193	Singlet-A	H-10->LUMO (14%), H-6->L+5 (57%)
59	41873.4	238.8	0.0137	Singlet-A	H-10->LUMO (12%), H-7->L+4 (11%), HOMO->L+8 (39%)
60	41887.1	238.7	0.0120	Singlet-A	H-10->LUMO (13%), H-7->L+4 (40%), H-6->L+5 (20%)
61	42149.2	237.3	0.0084	Singlet-A	H-7->L+5 (90%)
62	42241.2	236.7	0.0360	Singlet-A	H-11->LUMO (38%), H-10->LUMO (20%), H-8->L+2 (12%)
63	42545.2	235.0	0.0317	Singlet-A	H-11->L+1 (46%), H-8->L+2 (26%)
64	43126.8	231.9	0.0169	Singlet-A	H-11->L+2 (70%), H-8->L+1 (11%)
65	43226.8	231.3	0.0733	Singlet-A	HOMO->L+10 (28%)
66	43317.1	230.9	0.0176	Singlet-A	H-1->L+8 (44%)
67	43438.1	230.2	0.0025	Singlet-A	H-9->L+1 (52%), H-8->L+1 (11%)
68	43839.8	228.1	0.0378	Singlet-A	H-10->L+1 (20%), H-3->L+6 (10%)
69	44018.8	227.2	0.0415	Singlet-A	H-10->L+1 (25%), H-3->L+7 (11%), H-1->L+8 (11%)
70	44343.1	225.5	0.0129	Singlet-A	H-13->LUMO (32%), H-12->LUMO (33%)
71	44462.4	224.9	0.0024	Singlet-A	H-8->L+3 (51%)
72	44543.1	224.5	0.0056	Singlet-A	H-9->L+2 (43%), H-8->L+2 (13%), H-8->L+3 (13%)
73	44692.3	223.8	0.0285	Singlet-A	H-13->LUMO (20%), H-12->LUMO (31%), H-12->L+1 (10%)
74	44810.1	223.2	0.0047	Singlet-A	H-13->L+1 (13%), HOMO->L+11 (14%)
75	44998.0	222.2	0.0061	Singlet-A	H-10->L+2 (35%), H-9->L+2 (14%)
76	45016.5	222.1	0.0055	Singlet-A	H-13->LUMO (28%), H-13->L+1 (29%)
77	45232.7	221.1	0.0850	Singlet-A	H-1->L+10 (24%), HOMO->L+10 (12%)
78	45567.4	219.5	0.0125	Singlet-A	H-13->L+2 (12%), H-3->L+6 (14%), H-3->L+7 (10%), H-2->L+6 (12%), H-2->L+7 (10%), HOMO->L+11 (13%)
79	45764.2	218.5	0.0366	Singlet-A	H-3->L+6 (11%), H-2->L+6 (13%), HOMO->L+11 (15%), HOMO->L+12 (17%)
80	45910.2	217.8	0.0408	Singlet-A	H-13->L+2 (16%), HOMO->L+12 (14%)
81	46011.0	217.3	0.0487	Singlet-A	H-11->L+3 (41%), H-10->L+3 (12%)
82	46115.9	216.8	0.0793	Singlet-A	H-2->L+6 (11%), HOMO->L+10 (15%), HOMO->L+12 (17%)
83	46127.2	216.8	0.0170	Singlet-A	H-11->L+3 (10%), H-8->L+4 (38%)
84	46278.8	216.1	0.0016	Singlet-A	H-9->L+3 (57%), H-8->L+3 (12%)
85	46382.8	215.6	0.0228	Singlet-A	H-13->L+1 (10%), H-12->L+1 (27%), H-1->L+11 (10%)
86	46546.6	214.8	0.0070	Singlet-A	H-13->L+2 (17%), H-12->L+1 (21%), H-1->L+11 (18%)
87	46732.9	214.0	0.1272	Singlet-A	H-3->L+6 (13%), H-3->L+7 (12%), H-2->L+7 (13%)
88	46855.5	213.4	0.0482	Singlet-A	H-11->L+3 (15%), H-10->L+3 (19%)
89	46933.7	213.1	0.0065	Singlet-A	H-10->L+3 (19%), H-3->L+8 (10%), H-2->L+6 (14%), H-2->L+8 (10%)
90	46999.9	212.8	0.0044	Singlet-A	H-8->L+5 (70%)
91	47114.4	212.2	0.1021	Singlet-A	H-14->LUMO (23%)
92	47268.4	211.6	0.0267	Singlet-A	H-14->LUMO (41%), H-1->L+11 (11%)
93	47349.1	211.2	0.0348	Singlet-A	H-3->L+8 (12%), H-1->L+12 (22%)
94	47585.4	210.1	0.0028	Singlet-A	H-13->L+2 (18%), H-12->L+2 (59%)
95	47660.4	209.8	0.0184	Singlet-A	H-11->L+4 (46%), H-10->L+4 (12%)
96	47731.4	209.5	0.0511	Singlet-A	H-4->L+6 (14%), H-2->L+9 (15%)
97	47933.9	208.6	0.0360	Singlet-A	H-14->L+1 (25%)
98	48118.6	207.8	0.0621	Singlet-A	H-16->LUMO (16%), H-4->L+7 (13%), H-2->L+8 (13%)
99	48218.6	207.4	0.0052	Singlet-A	H-15->LUMO (37%), H-15->L+1 (13%), H-11->L+4 (10%)
100	48252.5	207.2	0.0040	Singlet-A	H-17->LUMO (32%)

Table S7: S_0 coordinates of complex 2.

Center Number	Atomic Number	Atomic Type	Coordinates (Angstroms)		
			X	Y	Z
1	6	0	1.37009	-0.901917	-1.452015
2	6	0	1.321067	-0.563041	-2.811801
3	1	0	0.688899	0.25654	-3.141157
4	6	0	2.073185	-1.260093	-3.764266
5	1	0	2.011938	-0.977262	-4.810159
6	6	0	2.909035	-2.315914	-3.377404
7	1	0	3.493845	-2.851221	-4.115984
8	6	0	2.980929	-2.674278	-2.033825
9	1	0	3.625046	-3.494685	-1.736332
10	6	0	2.219676	-1.976243	-1.078581
11	6	0	2.200761	-2.322022	0.348756
12	6	0	2.910499	-3.376071	0.943741
13	1	0	3.556659	-3.993782	0.335838
14	6	0	2.777101	-3.626485	2.304478
15	1	0	3.324048	-4.438206	2.767156
16	6	0	1.922364	-2.82047	3.063129
17	1	0	1.78102	-2.98429	4.122529
18	6	0	1.24325	-1.788204	2.428534
19	1	0	0.570916	-1.139038	2.972624
20	6	0	2.041869	1.25227	0.142249
21	6	0	3.26968	1.056342	0.789341
22	1	0	3.462435	0.123839	1.312007
23	6	0	4.263107	2.043113	0.779311
24	1	0	5.203645	1.865426	1.290365
25	6	0	4.050711	3.256804	0.114481
26	1	0	4.819193	4.020628	0.109046
27	6	0	2.841859	3.476791	-0.541476
28	1	0	2.680069	4.418329	-1.054506
29	6	0	1.845026	2.484523	-0.531444
30	6	0	0.544734	2.639896	-1.204017
31	6	0	0.154632	3.753299	-1.961646
32	1	0	0.834381	4.586004	-2.07625
33	6	0	-1.098619	3.782866	-2.564351
34	1	0	-1.403213	4.641421	-3.149611
35	6	0	-1.950892	2.688519	-2.402631
36	1	0	-2.937124	2.654009	-2.844701
37	6	0	-1.519537	1.60756	-1.64228

38	1	0	-2.17307	0.758127	-1.507059
39	6	0	-2.057929	-2.027909	-0.510394
40	6	0	-3.376822	-2.180034	-0.854189
41	1	0	-3.727608	-3.065663	-1.366952
42	6	0	-3.820287	-0.205487	0.761855
43	1	0	-4.490585	0.365605	1.388199
44	6	0	-2.460657	-0.217432	0.948494
45	6	0	-1.843581	0.633305	2.008296
46	6	0	-2.55811	1.137463	3.102887
47	1	0	-3.60408	0.89585	3.225682
48	6	0	-1.905697	1.932831	4.040044
49	1	0	-2.444258	2.320564	4.895218
50	6	0	-0.549938	2.218749	3.861411
51	1	0	-0.005185	2.83639	4.562154
52	6	0	0.10133	1.685276	2.755032
53	1	0	1.150414	1.875627	2.566226
54	6	0	-1.071706	-3.108281	-0.908571
55	1	0	-1.599994	-3.965984	-1.331615
56	1	0	-0.493582	-3.432502	-0.038106
57	1	0	-0.368852	-2.723823	-1.651711
58	7	0	1.380498	-1.533318	1.111047
59	7	0	-0.306801	1.578351	-1.051621
60	7	0	-0.525699	0.902478	1.85428
61	7	0	-1.566361	-0.987443	0.241718
62	8	0	-4.369295	0.07464	-1.786805
63	8	0	-5.862406	-1.390652	-0.420629
64	16	0	-4.491049	-0.893889	-0.661231
65	77	0	0.440535	0.010956	0.10272

Table S8: T_1 coordinates of complex 2.

Center Number	Atomic Number	Atomic Type	Coordinates (Angstroms)		
			X	Y	Z
1	6	0	1.383412	-1.015814	-1.371072
2	6	0	1.339398	-0.78081	-2.752111
3	1	0	0.684376	-0.008885	-3.14705
4	6	0	2.124872	-1.522216	-3.642527
5	1	0	2.067241	-1.321422	-4.707388
6	6	0	2.989364	-2.5184	-3.169359
7	1	0	3.599414	-3.087911	-3.860364
8	6	0	3.058279	-2.77283	-1.801904
9	1	0	3.725643	-3.546079	-1.43712
10	6	0	2.264035	-2.030134	-0.909531
11	6	0	2.239532	-2.268279	0.54005
12	6	0	2.974595	-3.248976	1.22365
13	1	0	3.647738	-3.891729	0.673643
14	6	0	2.832753	-3.394253	2.598646
15	1	0	3.39918	-4.149499	3.128697
16	6	0	1.946632	-2.557619	3.286049
17	1	0	1.801244	-2.642402	4.354101
18	6	0	1.243399	-1.599534	2.56782
19	1	0	0.54693	-0.92296	3.04563
20	6	0	2.03488	1.235273	0.077992
21	6	0	3.259103	1.081675	0.741735
22	1	0	3.449007	0.189942	1.331577
23	6	0	4.253943	2.06412	0.667316
24	1	0	5.191315	1.921325	1.194656
25	6	0	4.046884	3.22826	-0.081851
26	1	0	4.816901	3.988404	-0.137926
27	6	0	2.841211	3.403825	-0.75621
28	1	0	2.683578	4.307175	-1.334638
29	6	0	1.841708	2.416998	-0.679472
30	6	0	0.54206	2.533082	-1.36049
31	6	0	0.158427	3.598151	-2.188563
32	1	0	0.844223	4.415869	-2.359366
33	6	0	-1.095778	3.598289	-2.787838
34	1	0	-1.395754	4.418197	-3.428158
35	6	0	-1.957879	2.525197	-2.550847
36	1	0	-2.944596	2.47598	-2.990382
37	6	0	-1.533085	1.49297	-1.722555

38	1	0	-2.192037	0.660472	-1.523007
39	6	0	-1.992564	-2.071954	-0.413712
40	6	0	-3.279288	-2.263909	-0.832412
41	1	0	-3.562288	-3.129482	-1.415209
42	6	0	-3.866777	-0.360952	0.884076
43	1	0	-4.559903	0.254075	1.441311
44	6	0	-2.436506	-0.159087	0.992252
45	6	0	-1.890038	0.862694	1.817153
46	6	0	-2.660956	1.684367	2.702129
47	1	0	-3.735928	1.5748	2.740365
48	6	0	-2.036081	2.601814	3.513212
49	1	0	-2.620112	3.216996	4.187637
50	6	0	-0.62583	2.740596	3.463552
51	1	0	-0.103221	3.450527	4.089277
52	6	0	0.073495	1.94885	2.56579
53	1	0	1.148707	2.040249	2.458337
54	6	0	-0.97002	-3.145348	-0.719615
55	1	0	-1.469456	-4.041018	-1.09552
56	1	0	-0.413083	-3.399375	0.186948
57	1	0	-0.255336	-2.793073	-1.465287
58	7	0	1.388149	-1.450756	1.234691
59	7	0	-0.31566	1.490472	-1.138852
60	7	0	-0.514502	1.042729	1.761895
61	7	0	-1.548568	-0.956543	0.275844
62	8	0	-4.551955	-0.094995	-1.633409
63	8	0	-5.786014	-1.766877	-0.223238
64	16	0	-4.509712	-1.094515	-0.531197
65	77	0	0.426239	-0.003774	0.117901

References.

- (1). M. Nonoyama, *Bull. Chem. Soc. Jpn.*, 1974, **47**, 767-768.
- (2). G. A. Crosby and J. N. Demas, *J. Phys. Chem.*, 1971, **75**, 991-1024.
- (3). H. Ishida, S. Tobita, Y. Hasegawa, R. Katoh and K. Nozaki, *Coord. Chem. Rev.*, 2010, **254**, 2449-2458.
- (4). W. H. Melhuish, *J. Phys. Chem.*, 1961, **65**, 229-235.
- (5). N. G. Connelly and W. E. Geiger, *Chem. Rev.*, 1996, **96**, 877-910.
- (6). M. J. Frisch, G. W. Trucks, H. B. Schlegel, G. E. Scuseria, M. A. Robb, J. R. Cheeseman, G. Scalmani, V. Barone, B. Mennucci, G. A. Petersson, H. Nakatsuji, M. Caricato, X. Li, H. P. Hratchian, A. F. Izmaylov, J. Bloino, G. Zheng, J. L. Sonnenberg, M. Hada, M. Ehara, K. Toyota, R. Fukuda, J. Hasegawa, M. Ishida, T. Nakajima, Y. Honda, O. Kitao, H. Nakai, T. Vreven, J.

- Montgomery, J. A., J. E. Peralta, F. Ogliaro, M. Bearpark, J. J. Heyd, E. Brothers, K. N. Kudin, V. N. Staroverov, R. Kobayashi, J. Normand, K. Raghavachari, A. Rendell, J. C. Burant, S. S. Iyengar, J. Tomasi, M. Cossi, N. Rega, J. M. Millam, M. Klene, J. E. Knox, J. B. Cross, V. Bakken, C. Adamo, J. Jaramillo, R. Gomperts, R. E. Stratmann, O. Yazyev, A. J. Austin, R. Cammi, C. Pomelli, J. W. Ochterski, R. L. Martin, K. Morokuma, V. G. Zakrzewski, G. A. Voth, P. Salvador, J. J. Dannenberg, S. Dapprich, A. D. Daniels, Ö. Farkas, J. B. Foresman, J. V. Ortiz, J. Cioslowski and D. J. Fox, Gaussian Inc., Wallingford, CT, 2009.
- (7). (a) P. Hohenberg and W. Kohn, *Phys. Rev.*, 1964, **B136**, 864; (b) W. Kohn and L. Sham, *J. Phys. Rev.*, 1965, **A140**, 1133; (c) in *The Challenge of d and f Electrons*, eds. D. R. Salahub and M. C. Zerner, ACS, Washington, DC, 1989; (d) R. G. Parr and W. Yang, *Density-functional theory of atoms and molecules*, Oxford Univ. Press, Oxford, 1989.
- (8). (a) R. E. Stratmann, G. E. Scuseria and M. J. Frisch, *J. Chem. Phys.*, 1998, **109**, 8218; (b) R. Bauernschmitt and R. Ahlrichs, *Chem. Phys. Lett.*, 1996, **256**, 454; (c) M. E. Casida, C. Jamorski, K. C. Casida and D. R. Salahub, *J. Chem. Phys.*, 1998, **108**, 4439.
- (9). (a) A. D. Becke, *J. Chem. Phys.*, 1993, **98**, 5648-5652; (b) C. Lee, W. Yang and R. G. Parr, *Phys. Rev. B*, 1988, **37**, 785-789; (c) B. Miehlich, A. Savin, H. Stoll and H. Preuss, *Chem. Phys. Lett.*, 1989, **157**, 200-206.
- (10). V. A. Rassolov, J. A. Pople, M. A. Ratner and T. L. Windus, *J. Chem. Phys.*, 1998, **109**, 1223-1229.
- (11). (a) J. S. Binkley, J. A. Pople and W. J. Hehre, *J. Am. Chem. Soc.*, 1980, **102**, 939; (b) M. S. Gordon, J. S. Binkley, J. A. Pople, W. J. Pietro and W. J. Hehre, *J. Am. Chem. Soc.*, 1982, **104**, 2797; (c) W. J. Pietro, M. M. Francl, W. J. Hehre, D. J. Defrees, J. A. Pople and J. S. Binkley, *J. Am. Chem. Soc.*, 1982, **104**, 5039; (d) K. D. Dobbs and W. J. Hehre, *J. Comput. Chem.*, 1986, **7**, 359; (e) K. D. Dobbs and W. J. Hehre, *J. Comput. Chem.*, 1987, **8**, 861; (f) K. D. Dobbs and W. J. Hehre, *J. Comput. Chem.*, 1987, **8**, 880.
- (12). (a) W. J. Stevens, W. J. Basch and M. Krauss, *J. Chem. Phys.*, 1984, **81**, 6026; (b) W. J. Stevens, M. Krauss, H. Basch and P. G. Jasien, *Can. J. Chem.*, 1992, **70**, 612; (c) T. R. Cundari and W. J. Stevens, *J. Chem. Phys.*, 1993, **98**, 5555-5565.
- (13). (a) S. Ladouceur, D. Fortin and E. Zysman-Colman, *Inorg. Chem.*, 2010, **49**, 5625-5641; (b) M. S. Lowry, W. R. Hudson, R. A. Pascal Jr. and S. Bernhard, *J. Am. Chem. Soc.*, 2004, **126**, 14129-14135.
- (14). N. M. O'Boyle, *GaussSum 2.0*, Dublin City University; Dublin Ireland, 2006.
- (15). (a) S. Miertuš, E. Scrocco and J. Tomasi, *Chem. Phys.*, 1981, **55**, 117-129; (b) J. Tomasi, B. Mennucci and R. Cammi, *Chem. Rev.*, 2005, **105**, 2999-3094.